Surface-Dependent Kinetics of Cu(0)-Wire-Catalyzed Single-Electron Transfer Living Radical Polymerization of Methyl Acrylate in DMSO at 25 °C

Nga H. Nguyen, Brad M. Rosen, Gerard Lligadas, and Virgil Percec*

Roy & Diana Vagelos Laboratories, Department of Chemistry, University of Pennsylvania, Philadelphia, Pennsylvania 19104-6323

Received December 24, 2008; Revised Manuscript Received February 26, 2009

ABSTRACT: The effect of Cu(0) wire dimensions on the Cu(0) wire/Me_6-TREN-catalyzed heterogeneous single-electron transfer living radical polymerization (SET-LRP) of methyl acrylate (MA) initiated with methyl 2-bromopropionate (MBP) in DMSO at 25 °C was analyzed by kinetic experiments. These kinetic results were compared with those of Cu(0) powder/Me_6-TREN-catalyzed SET-LRP. Both wire and powder produce perfect SET-LRP with a first-order rate of polymerization in growing species up to 100% conversion. Nevertheless, Cu(0) wire experiments demonstrated SET-LRP with greater perfection, allowing for the accurate determination of the external rate order (vis-à-vis surface area) for heterogeneous Cu(0) catalyst and accurate prediction of k_p^{app} from wire dimension. Cu(0) wire also exhibited a significantly greater control of molecular weight distribution than Cu(0) powder. The combined advantages of easier catalyst preparation, handling, predictability, tunability, simple recovery/recycling, and enhanced control of molecular weight distribution make Cu(0)-wire-catalyzed SET-LRP the ideal methodology for the synthesis of tailored polyacrylates.

Introduction

Single-electron transfer living radical polymerization (SET-LRP)[1−3] has emerged as a powerful tool for the rapid synthesis of tailored and functional[4] polymers with excellent control of molecular weight, molecular weight distribution, perfect chain end fidelity,[5,6] and ultrahigh molecular weight. In SET, Cu(0)[1,7,8] and other electron-donor species such as Cu_2O, Cu_2S, Cu_2Se, and Cu_2Te[1−3] in the presence of a diversity of disproportionating N-containing ligands and solvents mediate an ultrafast living[9,10] radical polymerization[11−13] of vinyl monomers including methyl acrylate (MA),[1] methyl methacrylate (MMA),[1] ethyl acrylate (EA),[14] *n*-butyl acrylate (BA),[1,14] and vinyl chloride (VC)[1,2] without the need for the purification of the monomer, solvent, and final polymer.[15] In the absence of disproportionation, Cu(0)[7,8,16,17] and Ni(0)[11,18,19] mediate normal metal-catalyzed LRP[7,8,11−13] or a nonliving radical polymerization.[20,21] The activation step in SET-LRP is a low activation energy heterogeneous process that mediates heterolytic C−X bond cleavage.[22,23] Critical to SET-LRP is the disproportionation of the in situ generated Cu(I)X into Cu(0) activator and Cu(II)X_2 deactivator. The active Cu(0) catalyst is constantly regenerated via disproportionation. Simultaneously, disproportionation generates sufficient levels of Cu(II)X_2 deactivator without the need for bimolecular termination. In the case of ATRP,[13] bimolecular termination is responsible for the creation of the persistent radical effect.[24,25] Disproportionation of Cu(I)X is mediated by a synergy of N-containing ligands that stabilize Cu(II)X_2[26] such as Me_6-TREN, TREN, and PEI and polar solvents such as DMSO and other dipolar aprotic solvents, alcohols,[14] ionic liquids,[27] and water. Certain polar solvents such as MeCN[20] and nonpolar solvents such as toluene[28] do not readily facilitate disproportionation to the extent necessary to achieve a living polymerization. However, preliminary results suggested that outer-sphere electron transfer via caged Cu(I)X/NH_2-Capten[29] can mediate polymerization in toluene. Moreover, recent results have demonstrated that the addition of polar phenol additives[15,30] can enhance disproportionation in toluene allowing for SET-LRP. This confirms an earlier assumption that low levels of water in many commercial solvents could also mediate the disproportionation although to a lesser extent.[31]

Bulk Cu(0) and the nascent Cu(0) regenerated in situ via disproportion is thought to mediate the activation step in SET-LRP. The role of Cu(0) as the predominant activator in SET-LRP was recently confirmed.[21] It was demonstrated that the apparent rate constant of propagation, k_p^{app}, scales appropriately with the approximate surface area of Cu(0) utilized. Further, removal of the Cu(0) surface from contact with the SET-LRP reaction medium resulted in a complete interruption of the polymerization which could only be reversed by returned contact of the Cu(0) surface with the reaction medium. These observations indicated that SET-LRP is mediated by the Cu(0) surface[32−34] and not by dissolved Cu(I)X species and that reaction kinetics could be manipulated by the control of the total Cu(0) surface area used. Furthermore, in powder experiments incomplete consumption of Cu(0) is observed. This results in Cu(II)X_2 concentrations much less than 7.5×10^{-4} M. In studies by another group, comproportionation of Cu(II)X_2 and Cu(0) slowly plateaued to a concentration of 7.5×10^{-4} M after 1000 min.[35] This indicates that under our polymerization conditions Cu(0) does not reduce Cu(II)X_2 into Cu(I)X.

In this report, the previous study on surface effects of heterogeneous Cu(0) catalysts inspired the replacement of Cu(0) powder with Cu(0) wire. Cu(0) wire is a more convenient and cost-effective Cu(0) source that allows for greater variability and control of total surface area. Through a rigorous study of the kinetics of SET-LRP of MA initiated by methyl 2-bromopropionate (MBP) and catalyzed by Cu(0)/Me_6-TREN in DMSO at 25 °C utilizing various Cu(0) wire sources, it is definitively demonstrated that k_p^{app} scales appropriately with the total surface area of Cu(0) used. More important, we report here the unexpected discovery that switching from Cu(0) powder to Cu(0) wire results in a much greater control of polymer molecular weight distribution. The more facile tuning and subsequent removal and recycling of the Cu(0) wire and the enhanced control of molecular weight distribution make Cu(0) wire an ideal catalytic platform for the synthesis of tailored linear polymers and of polymers with complex architecture.[36−39]

* To whom correspondence should be addressed. E-mail: percec@sas.upenn.edu.

10.1021/ma8028562 CCC: $40.75
Published on Web 03/17/2009

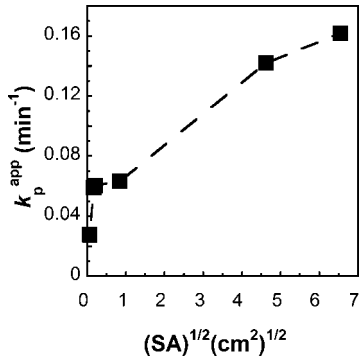

Figure 1. Relationship between the square root of the total surface area, $(SA)^{1/2}$, and the observed rate constant of propagation, k_p^{app}, of Cu(0) powder/Me_6-TREN-catalyzed SET-LRP of MA initiated with MBP in DMSO at 25 °C. Reaction conditions: MA = 1 mL, DMSO = 0.5 mL, $[MA]_0$ = 7.4 mol/L, $[MA]_0/[MBP]_0/[Cu]_0/[Me_6\text{-TREN}]_0$ = 222/1/0.1/0.1, and Cu (0) powder (diameters ranging from 425 μm to 50 nm). Adapted from ref 21.

Results and Discussion

Determination of External Order of Reaction for Cu(0) and the Effect of Cu(0) Wire Dimensions on the Kinetics of SET-LRP in DMSO at 25 °C. In a previous report[21] it was demonstrated that decreasing the diameter of the Cu(0) powder utilized for Cu(0) powder/Me_6-TREN catalyzed SET-LRP of MA in DMSO at 25 °C while maintaining the total mass of Cu(0) resulted in a monotonic increase in the observed k_p^{app}. Decreasing the diameter (d) of the Cu(0) powder increases its surface area (SA) to volume (V) ratio (SA/V) according to eq 1.

$$\frac{SA}{V} = \frac{6}{d} \tag{1}$$

One could then observe a linear relationship between the observed k_p^{app} and the square root of (SA/V). This is consistent with the previously determined 0. 51 rate order of $[Cu]_0$ powder reported for SET-LRP.[1] SA/V can be converted to an absolute total surface area (SA) by using eqs 2 and 3.

$$SA_{powder} = \left(\frac{SA}{V}\right)_{per\ particle}(\text{total } V) \tag{2}$$

$$SA_{powder} = \left(\frac{6}{d}\right)\left(\frac{m}{\rho}\right) = \left(\frac{6}{d}\right)\left(\frac{0.00032g}{8.96\ g\ cm^{-3}}\right) = \frac{0.000214\ cm^3}{d} \tag{3}$$

The same linear trend can then be observed, for the relationship between k_p^{app} and the square root of total surface area, $(SA)^{1/2}$ (Figure 1). The small deviation from linearity and the fact that extrapolation of the curve does not result in a k_p^{app} of 0 min^{-1} for 0 cm^2 SA are due to the polydispersity of commercial Cu(0) powder that is prepared via atomization, electrolytic deposition, or gaseous reduction techniques.[40] In reductive CCl_4 degradation, which proceeds by the same SET mechanism as the heterogeneous activation step in SET-LRP, the rate of degradation scales with particle SA.[41] However, nanocopper has an unusually high rate of activation compared to slightly larger species.[21] This phenomenon is frequently encountered in zero-oxidation-state metal catalysis but poorly understood. In fact, catalytically inert bulk metals such as Au(0)[42] can be converted into highly active catalysts[43] for organic transformations[44−47] when dispersed in the nanoparticulate, colloidal, or cluster states.[48] The effects of even low levels of smaller diameter species in commercial Cu(0) powder cannot be ignored. These small Cu(0) species are far more active than the bulk material, and therefore, they are likely responsible for causing higher particle size Cu(0) powders to react faster than predicted.

The polydispersity inherent to Cu(0) powder and the associated limited accuracy of SA determination as well as the difficulty in removing and recycling fine Cu(0) powder from the reaction mixture during polymer purification can be solved by using Cu(0) wire as an alternative Cu(0) source. Table 1 shows the results of the kinetic experiments for the Cu(0) wire/Me_6-TREN-catalyzed SET-LRP of MA initiated with MBP in DMSO using various dimensions of Cu(0) wire. The molar ratio between monomer, initiator, and ligand was kept constant, $[MA]_0/[MBP]_0/[Me_6\text{-TREN}]_0$ = 222/1/0.1. The dimensions and mass of the Cu(0) wire were varied. For convenient reference on kinetic plots and in discussion, the thickness of Cu wire is indicated by its guage, according to the American Wire Guage (AWG) standard (eq 4). Five gauges 16, 18, 20, 24, and 30, in order of decreasing thickness, were tested. The actual thicknesses for these Cu wire are listed in Table 1, as are the lengths used and their associated masses and SAs. The SAs of the wire were calculated via the standard thickness (D_n) for each guage (n) and the wire length according to eqs 4 and 5.

$$D_n = 0.0005\ cm \times 25.4 \times 92^{(36-n/39} \tag{4}$$

$$SA_{wire} = \pi D_n L + \pi\left(\frac{D_n}{2}\right)^2 \tag{5}$$

The previous determination of the external rate order for $[Cu]_0$ was based upon powder studies.[1] Cu(0) wire due to its surface uniformity and monodispersity allows for a more accurate determination of rate order. Figure 2a depicts ln k_p^{app} vs ln $[Cu]_0$ in Cu(0) wire/Me_6-TREN-catalyzed SET-LRP of MA in DMSO at 25 °C. As described previously,[49] the fitted slope of this semilogarithmic plot is the rate order of $[Cu]_0$, in this case 0.33. With respect to ln $[Cu]_0$, there are significant deviations from linearity in the rate order determination (R^2 = 0.85). As the activation step in SET-LRP is heterogeneous and catalyzed by the Cu(0) surface, the total surface area of catalyst is expected to be more meaningful than the total weight or concentration of the catalyst. Cu from the interior of the wire is expected to be irrelevant to the catalytic process. Figure 2b depicts ln k_p^{app} vs ln SA_{Cu}. As expected, the substitution of surface area for concentration removes the significant deviations from the semilogarithmic plot (R^2 = 0.98), resulting in an external rate order of 0. 44 for the surface area of Cu(0). Figure 2d plots the k_p^{app} vs $(SA)^{0.44}$. These data are also listed in Table 1 for all kinetic experiments generated in this study. Figure 2c plots the k_p^{app} vs $(SA)^{0.44}$ for all kinetic experiments and overlaps the data collected for Cu(0) powder from the previous study.[21] An external rate order of less than unity is expected for a heterogeneous reaction where the rate-limiting step is the physical process of mass transfer to the surface. Such a process is expected if liquid−solid heterogeneous catalysis where the chemical process taking place on the surface has a very low activation barrier, such as the activation step in SET-LRP.[23] The complex mechanism of SET-LRP involving disproportionation of Cu(I)X into Cu(0) and $Cu(II)X_2$ deactivator may also contribute to the less-than-one external rate order for Cu(0) surface area.

As expected, k_p^{app} varied linearly with $(SA)^{0.44}$ (Figure 2d). The data fits along the same curve observed in Cu(0) powder studies (Figure 2c), indicating that the same surface catalyst that mediated activation in the case of Cu(0) powder is responsible for catalysis in the Cu(0) wire process. Comparison of wire and powder experiments demonstrate greater linearity in the k_p^{app} vs $(SA)^{0.44}$ for the wire process due to the greater

Table 1. Dependence of k_p^{app} on the Dimensions of the Cu(0) Wire in the SET-LRP of MA Initiated with MBP in DMSO at 25 °C[a]

no.	wire guage[b]	std D[c] (cm)	measured D[d] (cm)	wire length (cm)	mass[e] (mg)	SA (cm^2)	k_p^{app} (min^{-1})	conv (%)	time (min)	M_w/M_n	M_w/M_n (90%)[f]
1	16	0.129	0.130	3.3	4.81	1.39	0.045	85.8	46	1.19	1.17
2	16	0.129	0.130	6.4	9.34	2.65	0.058	90.8	45	1.19	1.19
3	16	0.129	0.130	14.8	21.59	6.05	0.073	88.9	31	1.18	1.18
4	16	0.129	0.130	27.0	39.38	110.0	0.114	85.4	18	1.18	1.16
5	18	0.102	0.104	4.2	3.83	1.38	0.045	88.4	50	1.23	1.22
6	18	0.102	0.104	15.5	14.14	5.02	0.079	89.0	29	1.22	1.22
7	18	0.102	0.104	29.0	26.44	9.36	0.099	83.5	19	1.26	1.23
8	20	0.0812	0.0820	4.5	2.60	1.17	0.041	90.4	60	1.20	1.20
9	20	0.0812	0.0820	10.0	5.78	2.57	0.051	89.0	45	1.19	1.19
10	20	0.0812	0.0820	12.5	7.22	3.21	0.066	90.2	37	1.17	1.17
11	20	0.0812	0.0820	15.0	8.69	3.85	0.071	90.6	41	1.15	1.15
12	20	0.0812	0.0820	30.0	17.34	7.67	0.082	91.0	30	1.20	1.20
13	24	0.0511	0.0518	3.0	0.69	0.49	0.027	86.7	77	1.21	1.20
14	24	0.0511	0.0518	4.0	0.91	0.65	0.035	86.5	60	1.23	1.21
15	24	0.0511	0.0518	8.4	1.92	1.36	0.044	86.5	47	1.26	1.24
16	30	0.0255	0.0261	4.0	0.23	0.32	0.021	88.6	105	1.28	1.27
17	30	0.0255	0.0261	180.0	10.26	14.40	0.132	86.8	16	1.27	1.25
18[g]	20	0.0812	0.0820	12.5	7.22	3.21	0.056	87.2	30	1.16	1.15

[a] Reaction conditions: MA = 1 mL, solvent= 0.5 mL, $[MA]_0$ = 7. 4 mol/L, $[MA]_0/[MBP]_0/[Me_6\text{-TREN}]_0$ = 222/1/0.1. [b] American wire guage, useful for purchasing in the US, and used hereafter as a substitute for wire D. [c] American Wire Guage standard diameter, used in all calculations. [d] For verification only. [e] Calculated from dimensions and density. [f] Extrapolated M_w/M_n at 90% conversion using eq 10. [g] $[MA]_0/[BPE]_0/[Me_6\text{-TREN}]_0$ = 444/1/0.2.

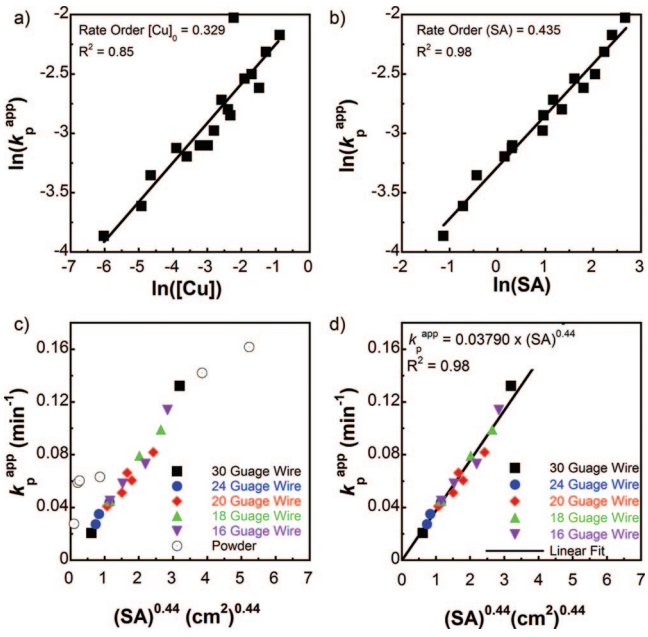

Figure 2. Determination of the external order of reaction in (a) $[Cu]_0$ and (b) surface area (SA) of Cu. Using 0.44 external order in surface area calculated in (b), (c) k_p^{app} vs $(SA)^{0.44}$ with superimposed powder experiments (Figure 1) and (d) k_p^{app} vs $(SA)^{0.44}$ with a linear regression fit through the origin for Cu(0) wire/Me_6-TREN-catalyzed SET-LRP of MA initiated with MBP in DMSO at 25 °C. Reaction conditions: MA = 1 mL, solvent (DMSO) = 0.5 mL, $[MA]_0$ = 7.4 mol/L, $[MA]_0/[MBP]_0/[Me_6\text{-TREN}]_0$ = 222/1/0.1.

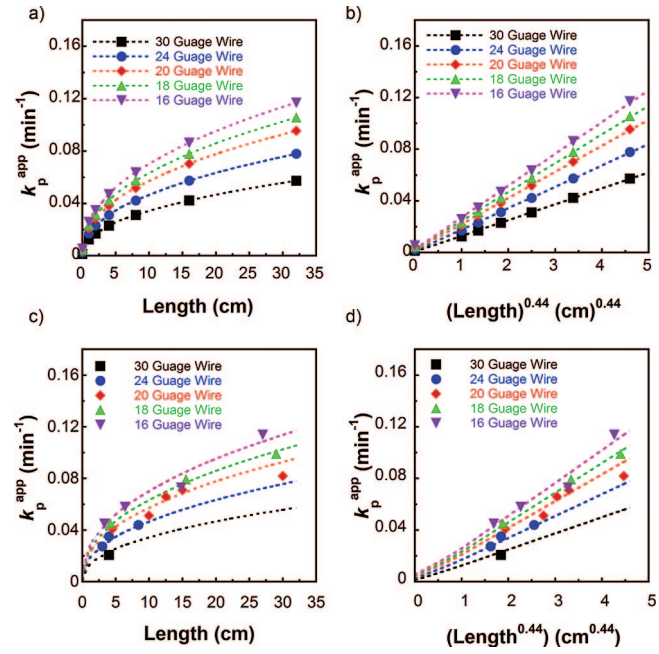

Figure 3. (a) Predicted k_p^{app} vs length, (b) k_p^{app} vs $(length)^{0.44}$, and (c/d) correspondence with experimental data for the Cu(0) wire/Me_6-TREN-catalyzed SET-LRP of MA initiated with MBP in DMSO at 25 °C for various wire thicknesses/guages. Reaction conditions: MA = 1 mL, solvent (DMSO) = 0.5 mL, $[MA]_0$ = 7.4 mol/L, $[MA]_0/[MBP]_0/[Me_6\text{-TREN}]_0$ = 222/1/0.1.

surface uniformity and monodispersity of Cu(0) wire. The same overall range in k_p^{app} is accessible with Cu(0) powder, but specifying the rate can be achieved more readily with Cu(0) wire via manipulation of the wire thickness and length. Linear regression of the k_p^{app} vs $(SA)^{0.44}$ for wire data (Figure 2c) reveals a simple relationship between k_p^{app} and $(SA)^{0.44}$ (eqs 6 and 7).

$$k_p^{app} = 0.03790 \times (SA)^{0.44} \quad (6)$$

$$k_p^{app} = 0.03790 \times \left(\pi D_n L + \pi\left(\frac{D_n}{2}\right)^2\right)^{0.44} \quad (7)$$

Equation 7 allows for the prediction of the k_p^{app} of a SET-LRP of MA in DMSO at 25 °C mediated by Cu(0) wire/Me_6-TREN, using the reaction conditions reported here. Changing the concentrations of $[MA]_0$, $[MBP]_0$, or $[DMSO]_0$ will modify the k_p^{app} according to the conventional kinetic equations of living radical polymerization. In practical terms, it is the length of Cu(0) wire that is measured and determined for each experiment. While this determines the $(SA)^{0.44}$, it is useful to be able to directly predict the k_p^{app} directly from wire length. Predicted k_p^{app} for typical wire lengths (Figure 3a) and 0.44 power of wire length (Figure 3b) can be extrapolated through the use of eq 7, the latter of which is pseudolinear. These predicted curves are in close agreement with experimental data (Figure 3c,d).

Comparison of the Molecular Weight Evolutions of Cu(0) Wire/Me_6-TREN-Catalyzed and Cu(0) Powder/Me_6-TREN-Catalyzed SET-LRP in DMSO at 25 °C. The use of Cu(0) wire as catalyst allows for greater ease in reaction rate

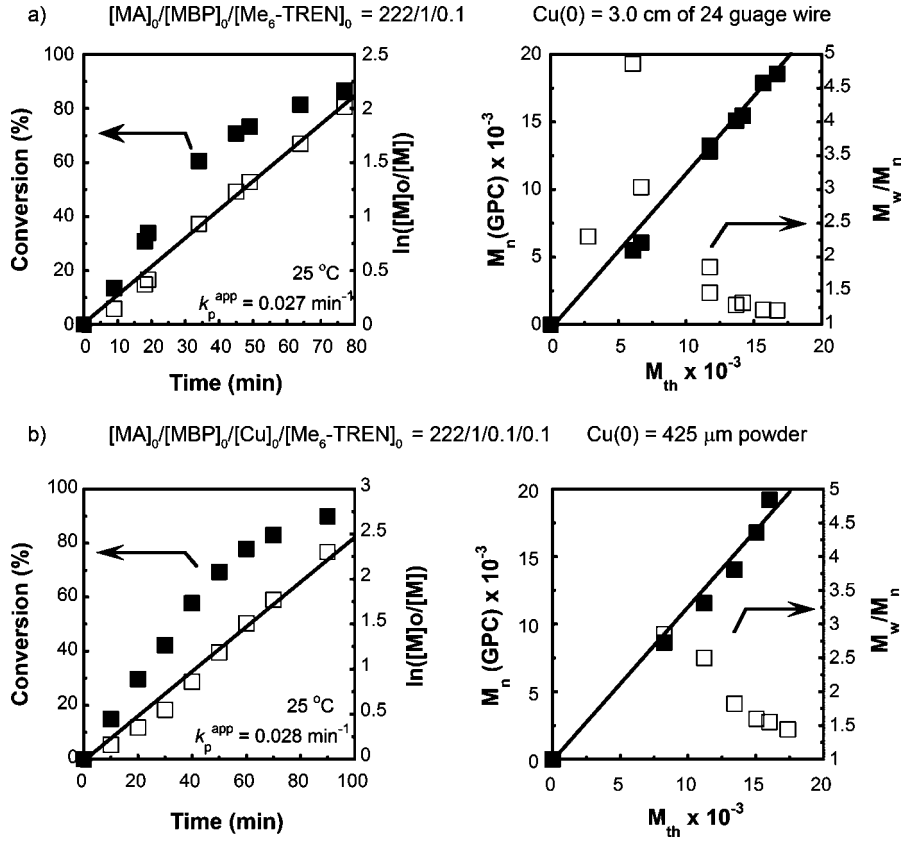

Figure 4. Comparison of low k_p^{app} domain SET-LRP of MA initiated with MBP in DMSO in 25 °C catalyzed with (a) Cu(0) wire and (b) Cu(0) powder. Reaction conditions: (a) MA = 1 mL, solvent (DMSO) = 0.5 mL, $[MA]_0 = 7.4$ mol/L, $[MA]_0/[MBP]_0/[Me_6\text{-TREN}]_0 = 222/1/0.1$. Cu = 3.0 cm of 24 guage wire. (b) MA = 1 mL, solvent (DMSO) = 0.5 mL, $[MA]_0 = 7.4$ mol/L, $[MA]_0/[MBP]_0/[Cu]_0/[Me_6\text{-TREN}]_0 = 222/1/0.1/0.1$. Cu = 425 μm.

tuning, catalyst preparation, removal, and recyclability. However, in order for Cu(0) wire to be a suitable replacement for Cu(0) powder SET-LRP, we need to ensure that the polymerization kinetics are living and provide good control of molecular weight evolution and distribution. In all kinetic plots, M_{th} is calculated according to eq 8, where q is conversion, MW^{MA} is the molar mass of the monomer MA, and MW^{I} is the molar mass of initiator. Since MW^{I} is small in comparison to polymer mass, M_{th} is proportional to conversion.

$$M_{th} = \frac{[M]_0}{[I]_0} \times MW^{MA} \times q + MW^{I} \quad (8)$$

Figures 4, 5, and 6 show the kinetic plots for Cu(0) wire/Me_6-TREN-catalyzed SET-LRP of MA in DMSO at 25 °C for slow ($k_p^{app} = 0.027$ min^{-1}), medium ($k_p^{app} = 0.067$ min^{-1}), and fast ($k_p^{app} = 0.132$ min^{-1}) polymerizations, respectively, and provide a comparison with Cu(0) powder/Me_6-TREN-catalyzed SET-LRP experiments with similarly observed k_p^{app} (0.027, 0.060, and 0.142 min^{-1}). In all cases Cu(0) wire/Me_6-TREN-catalyzed SET-LRP demonstrate the classic behavior of a living polymerization.[9,10] In fact, for each rate domain, the final M_w/M_n values for Cu(0) wire/Me_6-TREN-catalyzed SET-LRP are significantly lower than those observed in the corresponding Cu(0) powder experiments. For the low k_p^{app} domain (Figure 4), 3.0 cm of 24 gauge wire (Figure 4a), $k_p^{app} = 0.027$ min^{-1}, was compared to 425 μm powder (Figure 4b), $k_p^{app} = 0.028$ min^{-1}. The M_w/M_n at about 90% conversion for the Cu(0) wire (Figure 4a) was 1.21, while the final M_w/M_n value for the Cu(0) powder (Figure 4b) was 1.44. For the middle k_p^{app} domain (Figure 5), 12.5 cm of 20 gauge wire (Figure 5a), $k_p^{app} = 0.066$ min^{-1}, was compared to 45 μm powder (Figure 5b), $k_p^{app} = 0.060$ min^{-1}. The M_w/M_n at about 90% conversion for the Cu(0) wire (Figure 5a) was 1.17, while the final M_w/M_n value for the Cu(0) powder (Figure 4b) was 1.42. For the high k_p^{app} domain (Figure 6), 180 cm of 30 gauge wire (Figure 6a), $k_p^{app} = 0.132$ min^{-1}, was compared to 100 nm powder (Figure 6b), $k_p^{app} = 0.1421$ min^{-1}. The M_w/M_n at about 90% conversion for the Cu(0) wire (Figure 6a) was 1.27, while the final M_w/M_n value for the Cu(0) powder (Figure 6b) was 1.47.

Evolution of Chain-End Functionality. When Cu(0) wire/Me_6-TREN-catalyzed SET-LRP is used for the preparation of macroinitiators for block copolymers and for other polymers with complex architecture, it is necessary to consider the chain-end functionality of the resulting PMA samples. The evolution of the chain-end percentage functionality (f) (Figure 7a) was determined for a representative polymerization using 12.5 cm of 20 guage Cu(0) wire (Figure 5a). In a second polymerization, f was monitored through the withdrawal of samples from the reaction mixture at different times followed by their analysis by 500 MHz ^{1}H NMR. Figure 7b depicts the 500 MHz ^{1}H NMR spectrum together with its proton assignments of the isolated PMA sample ($M_n = 18\,326$ and $M_w/M_n = 1.1$, after 40 min at 89% monomer conversion). The signals of the protons of the main chain ($-CH_2-$ and $-CH-$) are present in the region 1.30−2.70 ppm. The signal of the $-OCHH_3$ side group appears at 3.7 ppm. The value of f can be estimated by a comparison of the integrals of peaks $\mathbf{H}_c$ (corresponding to the initiator $\mathbf{CH}_3-CH$ groups) and $\mathbf{H}_k$ (corresponding to the proton in the α-position of the bromine chain end) (eq 9).

$$\%\ \text{functionality}\ (f) = \left[\frac{\mathbf{H}_k}{\mathbf{H}_c/3}\right] \times 100 \quad (9)$$

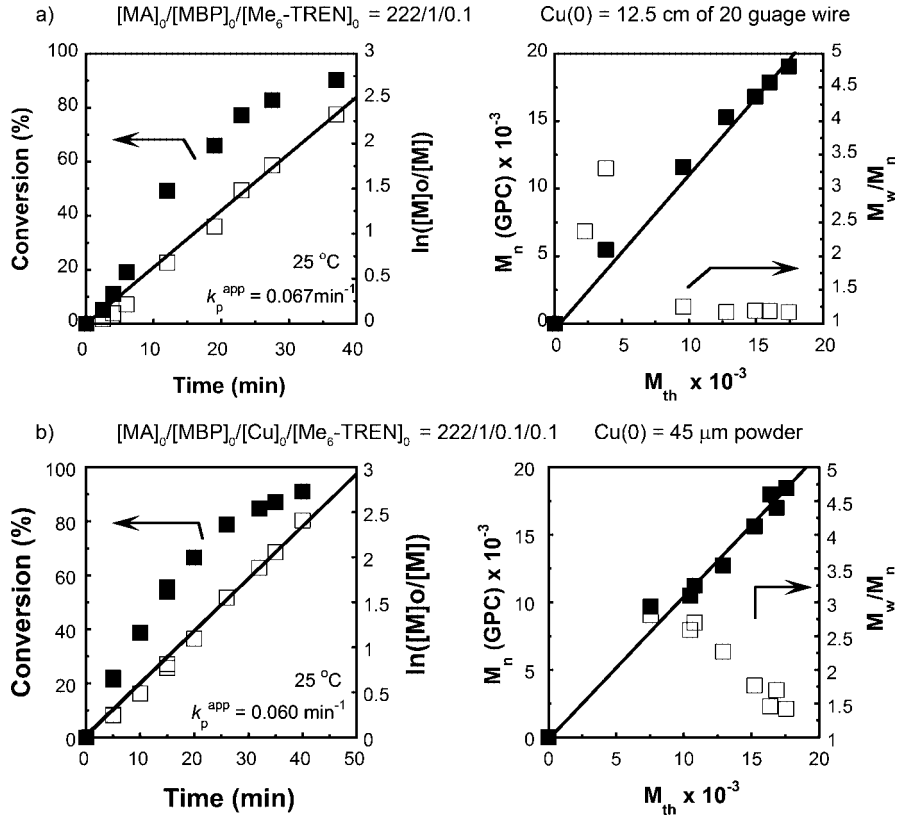

Figure 5. Comparison of middle k_p^{app} domain SET-LRP of MA initiated with MBP in DMSO in 25 °C catalyzed with (a) Cu(0) wire and (b) Cu(0) powder. Reaction conditions: (a) MA = 1 mL, solvent (DMSO) = 0.5 mL, $[MA]_0$ = 7.4 mol/L, $[MA]_0/[MBP]_0/[Me_6\text{-TREN}]_0$ = 222/1/0.1. Cu = 12.5 cm of 20 guage wire. (b) MA = 1 mL, solvent (DMSO) = 0.5 mL, $[MA]_0$ = 7.4 mol/L, $[MA]_0/[MBP]_0/[Cu]_0/[Me_6\text{-TREN}]_0$ = 222/1/0.1/0.1. Cu = 45 μm.

This value, measured by 500 MHz ^{1}H NMR, is the fraction of initiated chains that are effectively capped with a bromine atom. In the depicted Cu(0) wire experiment, f is extremely high throughout the polymerization, culminating in PMA sample with $f > 98\%$. This value is within the experimental error of our NMR method and confirms a polymer with perfect or nearly perfect retention of functional chain ends.[20] Cu(0) powder also exhibited $f > 98\%$ throughout the polymerization,[20] indicating that both wire and powder can be utilized in the synthesis of functionally terminated polymers.

Molecular Weight Distribution in the Cu(0) Wire/Me$_6$-TREN-Catalyzed SET-LRP of MA in DMSO at 25 °C. Increasing the targeted molecular weight,[1] use of a bifunctional initiator, or addition of CuX_2[50] has been shown to enhance the control of molecular weight distribution in SET-LRP of PMA. In a recent study,[21] using various particle sizes of Cu(0) and the starting reactants in a ratio of $[MA]_0/[MBP]_0/[Cu]_0/[Me_6\text{-TREN}]_0$ = 222/1/0.1/0.1 ($M_{th} \sim 20\,000$), M_w/M_n of roughly 1.35 was typically obtained at conversion of about 90%. Relatively high polydispersities of the resultant PMA samples could be due to the inherent polydispersity of the Cu(0) powder used in their preparation. The higher activity of nanosized copper present to varying degrees in commercial powders likely enhance the activation rate in a nonuniform fashion. As shown in the previous section, Cu(0) wire/Me$_6$-TREN-catalyzed SET-LRP of MA in DMSO at 25 °C effectively solves the problem of control in low molecular weight monofunctional PMA as evidenced by lower M_w/M_n (~1.15−1.20 for 90% conversion) than Cu(0) powder/Me$_6$-TREN-catalyzed SET-LRP. The k_p^{app} of Cu(0) wire/Me$_6$-TREN-catalyzed SET-LRP are comparable with those of Cu(0) powder, and therefore, the enhanced control of molecular weight distribution can be attributed to the uniformity of "monodisperse" wire.

Direct comparisons of M_w/M_n are meaningless, unless the samples being compared are at equivalent conversions. Therefore, we compared the values of M_w/M_n at 90% conversion. M_w/M_n at 90% conversion using the typical Poisson distribution for the evolution of the molecular weight distribution (eq 10), where q is conversion.

$$\frac{M_w}{M_n} = 1 + K_{SET\text{-}LRP}\left(\frac{2}{q} - 1\right) \qquad (10)$$

$K_{SET\text{-}LRP}$ is a value that correlates with the active concentration of radicals and is influenced by the total initiator concentration $[I]_0$, the total surface area of catalyst SA, and the absolute rate constants of activation (k_{act}), deactivation (k_d), and propagation (k_p). M_w/M_n at 90% conversion can be found for each each sample by first solving for $K_{SET\text{-}LRP}$ for the M_w/M_n and conversion, q, of each polymer sample from the kinetic studies. This $K_{SET\text{-}LRP}$ value can be used with q = 90% in eq 10 to extrapolate M_w/M_n at 90% conversion.

Contrary to conventional LRP[12] including ATRP,[13,51,52] M_w/M_n does not increase with k_p^{app}. Using 3.3 cm of 16 guage wire, polymerization with a $k_p^{app} = 0.045\ min^{-1}$ produced PMA with M_w/M_n = 1.17 at 90% conversion. Increasing the wire length to 27.0 cm of 16 guage wire, the polymerization rate more than doubled to $k_p^{app} = 0.114\ min^{-1}$. However, the resulting PMA had M_w/M_n = 1.16. Furthermore, unlike conventional LRP and ATRP,[51,52] there is no increase in M_w/M_n at very high conversion due to bimolecular termination when monomer concentration is low.

Cu(0) Wire/Me$_6$-TREN-Catalyzed SET-LRP of MA Initiated with BPE in DMSO at 25 °C. The use of monofunctional initiators such as MBP is useful for the synthesis of tailored

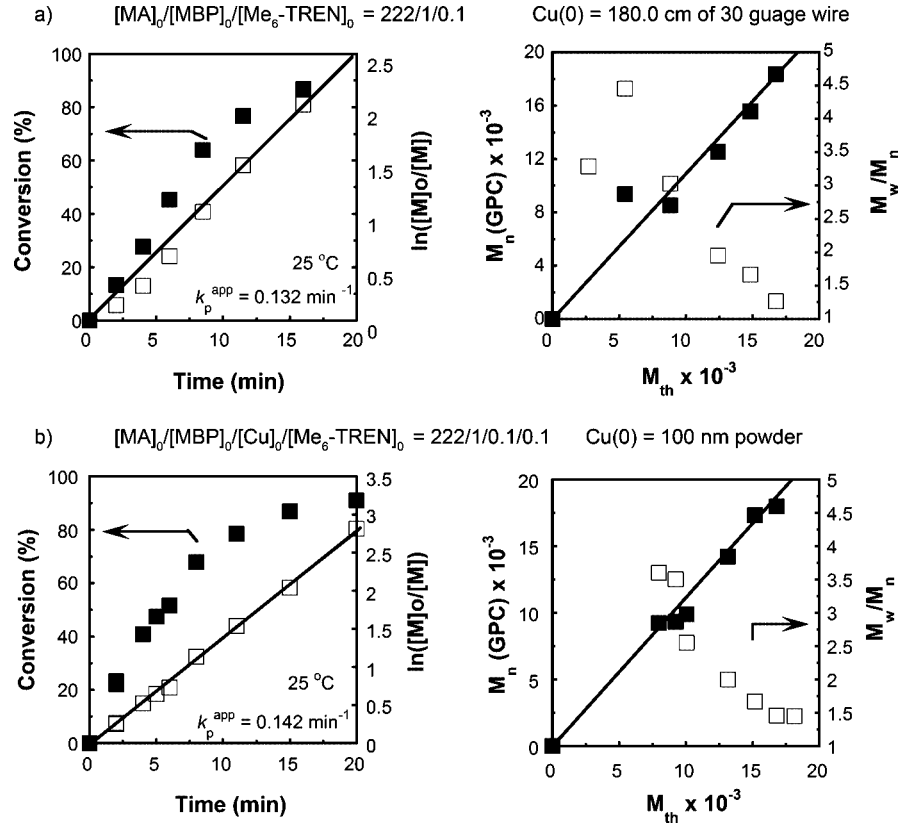

Figure 6. Comparison of middle k_p^{app} domain SET-LRP of MA initiated with MBP in DMSO in 25 °C catalyzed with (a) Cu(0) wire and (b) Cu(0) powder. Reaction conditions: (a) MA = 1 mL, solvent (DMSO) = 0.5 mL, $[MA]_0$ = 7.4 mol/L, $[MA]_0/[MBP]_0/[Me_6\text{-TREN}]_0$ = 222/1/0.1. Cu = 180 cm of 30 guage wire. (b) MA = 1 mL, solvent (DMSO) = 0.5 mL, $[MA]_0$ = 7.4 mol/L, $[MA]_0/[MBP]_0/[Cu]_0/[Me_6\text{-TREN}]_0$ = 222/1/0.1/0.1. Cu = 100 nm.

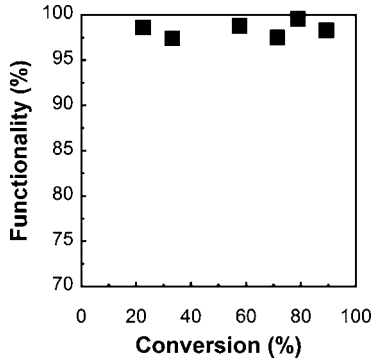

Figure 7. Percentage of bromine-functionalized chains vs conversion (%).

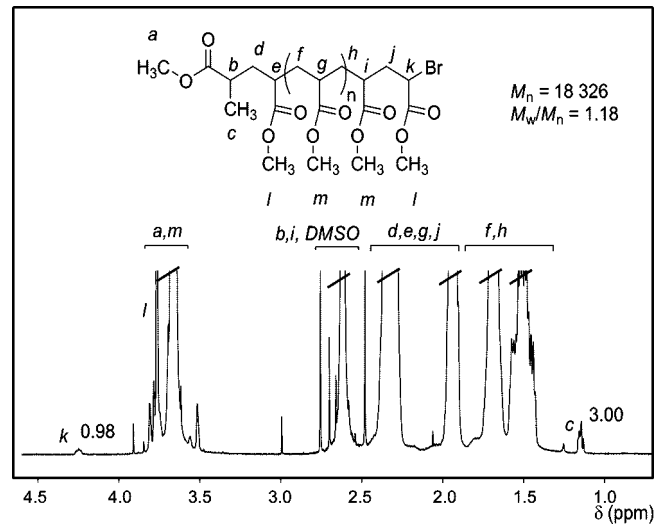

Figure 8. 500 MHz ^{1}H NMR spectrum ($CDCl_3$) of PMA obtained for the Cu(0) wire/Me_6-TREN-catalyzed SET-LRP of MA initiated with MBP in DMSO at 25 °C. MA = 1 mL, solvent (DMSO) = 0.5 mL, $[MA]_0$ = 7.4 mol/L, $[MA]_0/[MBP]_0/[Me_6\text{-TREN}]_0$ = 222/1/0.1. Cu = 12.5 cm of 20 guage wire.

homopolymers and AB block copolymers. The use of bifunctional initiators such as bis(2-bromopropionyloxy)ethane (BPE) is of particular interest in the synthesis of telechelic macroinitiators for ABA block copolymerization and for the synthesis of dendritic macromolecules via the TERMINI concept.[36−39] Further, in previous studies the use of a bifunctional initiator resulted in enhanced control of molecular weight distribution versus the monofunctional initiator, likely through the complete elimination of any secondary effects of bimolecular termination in the early stages of the polymerization.

Figure 9 compares the kinetics of Cu(0) wire/Me_6-TREN SET-LRP initiated with monofunctional (Figure 9a) and bifunctional initiators (Figure 9b). In both cases $[MA]_0$, $[Me_6\text{-TREN}]_0$, and $[DMSO]_0$ were kept the same, but as we switched from a monofunctional to a bifunctional initiator, the initiator concentration was halved to keep the chain end concentration the same. Thus, for the polymerization initiated with MBP, $[MA]_0/[MBP]_0/[Me_6\text{-TREN}]_0$ = 222/1/0.1, but for the polymerization initiated with BPE, $[MA]_0/[BPE]_0/[Me_6\text{-TREN}]_0$ = 444/1/0.2. For both polymerizations the same dimensions of Cu(0) wire were employed, specifically 12.5 cm of 20 guage wire. The polymerization initiated with MBP (Figure 9a) is fast with k_p^{app} of 0.066 min^{-1} but is very well controlled with a M_w/M_n of 1.17 (M_n = 19 068 at 90.2% conversion). The polymerization initiated with BPE occurs at a slightly lower rate k_p^{app}

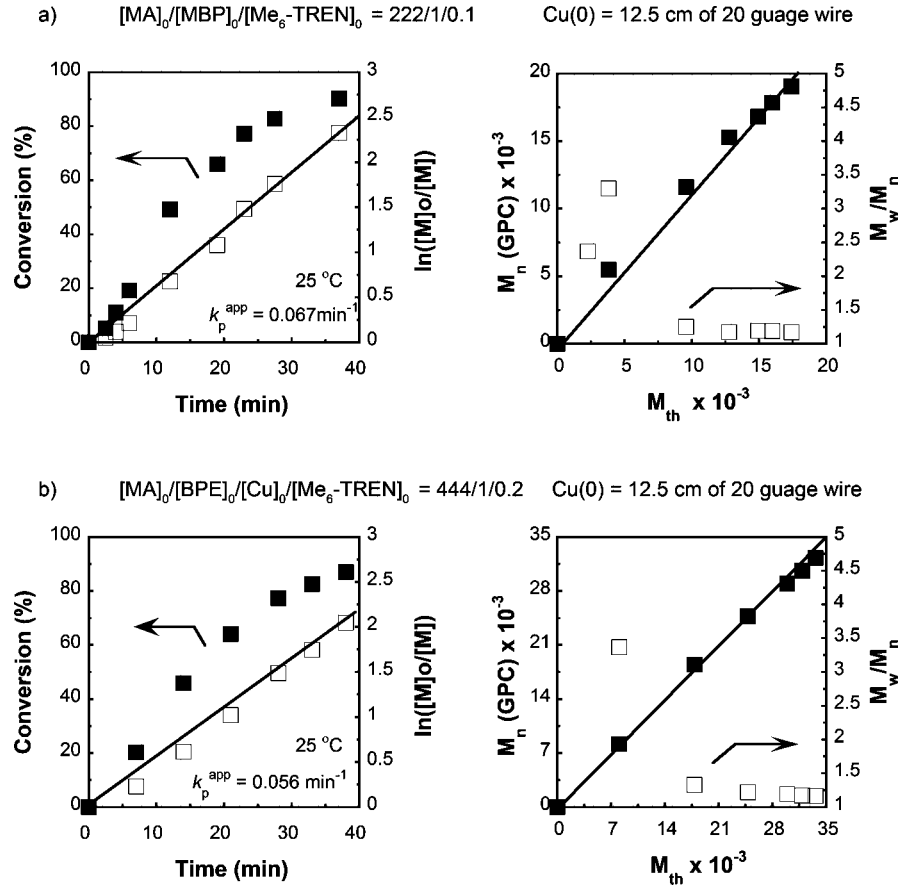

Figure 9. (a) Kinetic plots of SET-LRP of MA initiated by MBP and catalyzed by Cu(0) wire/Me_6-TREN in DMSO at 25 °C. Reaction conditions: MA = 1 mL, DMSO = 0.5 mL, $[MA]_0$ = 7.4 mol/L, $[MA]_0/[MBP]_0/[Me_6\text{-TREN}]_0$ = 222/1/0.1, and Cu(0) = 12.5 cm of 20 guage wire. (b) Kinetic plots of SET-LRP of MA initiated by BPE and catalyzed by Cu(0) wire/Me_6-TREN in DMSO at 25 °C. Reaction conditions: MA = 1 mL, DMSO = 0.5 mL, $[MA]_0$ = 7.4 mol/L, $[MA]_0/[BPE]_0/[Me_6\text{-TREN}]_0$ = 444/1/0. 2, and Cu(0) = 12.5 cm of 20 guage wire.

= 0.056 and marginally better control of molecular weight distribution, M_w/M_n = 1.16 (M_n = 32 290, at 87.2% conversion).

In both polymerizations each initiation site results in the production of a PMA chain with $M_n \sim 16\,000-19\,000$. However, in the case of the bifunctional initiator the initiator sites are connected, resulting in polymers with double M_n. Unlike with Cu(0) powder/Me_6-TREN-catalyzed SET-LRP, the use of a bifunctional initiator does not significantly enhance the control of molecular weight evolution.

Conclusions

In the Cu(0) wire/Me_6-TREN-catalyzed SET-LRP of MA initiated with MBP in DMSO at 25 °C, the total surface area Cu(0) directly affects the k_p^{app}. Increasing the surface from 0.32 to 14.40 cm^2 resulted in a an increase of k_p^{app} from 0.021 to 0.132 min^{-1}. These results fit the same trend observed with Cu(0) powder, indicating the same surface-mediated SET activation process. However, in the case of wire a greater linearity is observed. This is due to the lower polydispersity of Cu wire and allows for easy prediction of reaction rates from wire dimensions. The Cu(0)-wire-catalyzed SET-LRP also exhibits a greater control of molecular weight distribution. The ability to predict and tune the k_p^{app}, the easy preparation/removal/recycling of catalyst, the lack of coloration of the reaction mixture, and therefore the lack of need of purification of the resulting polymers, and the enhanced control of molecular weight distribution make Cu(0) wire/Me_6-TREN-catalyzed SET-LRP an improved method for the rapid and controlled synthesis of homopolymers, block copolymers, and polymers with complex architecture.[36−39]

Experimental Section

Materials. Methyl acrylate (MA) (99%, Aldrich), methyl 2-bromopropionate (MBP) (98%, Aldrich), acetonitrile (MeCN) (99.9%, Fisher), and Cu wire (16, 18, 20, and 24 guage from Fischer; 30 guage from Small Parts, Inc.) were used as received. The thickness of the Cu(0) wires was verified to be within 0.1−0.2 mm of the American Standard Wire system according to a Starret No. 230 Vernier Outside Micrometer. Dimethyl sulfoxide (DMSO) (99.9%, Fischer) was used as received or purified by vacuum distillation. Hexamethylated tris(2-aminoethyl)amine (Me_6-TREN) was synthesized as described in the literature.[53]

Techniques. 500 MHz ^{1}H NMR spectra were recorded on a Bruker DRX500 NMR instrument at 20 °C in $CDCl_3$ with tetramethylsilane (TMS) as internal standard. Gel permeation chromatographic (GPC) analysis of the polymer samples were done on a Perkin-Elmer Series 10 high-performance liquid chromatograph, equipped with an LC-100 column over (40 °C), a Nelson Analytical 900 Series integration data station, a Perkin-Elmer 785A UV−vis detector (254 nm), a Varian star 4090 refractive index (RI) detector, and two AM gel (500 Å, 5 μm and 10^4 Å, 5 μm) columns. THF (Fisher, HPLC grade) was used as eluent at a flow rate of 1 mL/min. The number-average (M_n) and weight-average (M_w) molecular weights of the PMA samples were determined with PMMA standards purchased from American Polymer Standards. Since the hydrodynamic volume of PMA is the same as of PMMA, no correction is needed in the determination of M_n.

Typical Procedure for Polymerization Kinetics. The monomer (MA, 1 mL, 11.1 mmol), solvent (DMSO, 0.5 mL), initiator (MBP, 5.6 μL, 0.05 mmol), catalyst (3.3 cm of guage 16 wire, wrapped around a Teflon-coated stirbar), and ligand (Me_6-TREN, 1.15 mg, 0.005 mmol) were added to a 25 mL Schlenk tube in the following

order: Cu(0), monomer, ligand, solvent, initiator. After six freeze−pump−thaw cycles, the tube was filled with nitrogen, and the reaction mixture was placed in an oil bath thermostated at 25 ± 0.1 °C with stirring. The side arm of the tube was purged with nitrogen before it was opened for samples to be removed at predetermined times, with an airtight syringe. Samples were dissolved in $CDCl_3$, and the conversion was measured by ^1H NMR spectroscopy. The M_n and M_w/M_n values were determined by GPC with PMMA standards (conversion: 86% (46 min), M_n(GPC) = 18 100, $M_w/M_n = 1.19$). The polymerization mixture was dissolved in 5 mL of CH_2Cl_2 and passed through a small basic Al_2O_3 chromatographic column to remove any residual nascent Cu(0) catalyst and Cu(II) deactivator, and the resulting solution was precipitated twice in 60 mL of cold methanol (about 0 °C) with stirring. Methanol was removed by decantation, and the final colorless polymer was dried under vacuum until constant weight was reached.

Chain-End Analysis of PMA. The evolution of percentage of functionality (*f*) of the PMA was monitored via withdrawal of samples from the polymerization mixture at different times followed by their analysis by 500 MHz ^1H NMR. The signals of all protons of the main chain (−CH_2− and −CH−) are present in the region 1.30−2.70 ppm. The signal of the −$OCHH_3$ side groups appears at around 3.7 ppm. Most important are the signals associated with the chain ends. The signal at 4.24 ppm corresponds to the proton located in the α-position of the bromine chaine end, $\mathbf{H}_k$, while the signal at 1.14 ppm, $\mathbf{H}_c$, is associated with the initiator $\mathbf{CH}_3$−CH− groups. The percentage of chain-end functionality of PMA can be estimated from the integral ratio between these two signals (eq 8). This value is the fraction of initiated chains that are effectively capped by a bromine atom.

Acknowledgment. Financial support by the National Science Foundation (DMR-0548559 and DMR-0520020) and the P. Roy Vagelos Chair at Penn is gratefully acknowledged. B.M.R. gratefully acknowledges funding from a NSF Graduate Research Fellowship and ACS Division of Organic Chemistry Graduate Fellowship (Roche).

Supporting Information Available: Monomer conversion and $\ln([M_0]_0/[M])$ vs time plots and molecular weight evolution plots for all other kinetic experiments in Table 1. This material is available free of charge via the Internet at http://pubs.acs.org.

References and Notes

(1) Percec, V.; Guliashvili, T.; Ladislaw, J. S.; Wistrand, A.; Stjerndahl, A.; Sienkowska, M. J.; Monteiro, M. J.; Sahoo, S. *J. Am. Chem. Soc.* **2006**, *128*, 14156–14165.
(2) Percec, V.; Popov, A. V.; Ramierez-Castillo, E.; Monteiro, M.; Barboiu, B.; Weichold, O.; Asandei, A. D.; Mitchell, C. M. *J. Am. Chem. Soc.* **2002**, *124*, 4940–4941.
(3) Percec, V.; Popov, A. V.; Ramirez-Castillo, E.; Weichold, O. *J. Polym. Sci., Part A: Polym. Chem.* **2003**, *41*, 3283–3299.
(4) Potisek, S. L.; Davis, D. A.; Sottos, N. R.; White, S. R.; Moore, J. S. *J. Am. Chem. Soc.* **2007**, *129*, 13808–13809.
(5) Lligadas, G.; Percec, V. *J. Polym. Sci., Part A: Polym. Chem.* **2007**, *45*, 4684–4695.
(6) Lligadas, G.; Ladislaw, J.; Guliashvili, T.; Percec, V. *J. Polym. Sci., Part A: Polym. Chem.* **2007**, *45*, 278–288.
(7) Percec, V.; Barboiu, B.; van der Sluis, M. *Macromolecules* **1998**, *31*, 4053–4056.
(8) van der Sluis, M.; Barboiu, B.; Pesa, N.; Percec, V. *Macromolecules* **1998**, *31*, 9409–9412.
(9) Szwarc, M. *Nature (London)* **1956**, *178*, 1168–1169.
(10) Szwarc, M.; Levy, M.; Milkovich, R. *J. Am. Chem. Soc.* **1956**, *78*, 2656–2657.
(11) Otsu, T. *J. Polym. Sci., Part A: Polym. Chem.* **2000**, *38*, 2121–2136.
(12) Kamigaito, M.; Ando, T.; Sawamoto, M. *Chem. Rev.* **2001**, *101*, 3689–3746.
(13) Matyjaszewski, K.; Xia, J. *Chem. Rev.* **2001**, *101*, 2921–2990.
(14) Lligadas, G.; Percec, V. *J. Polym. Sci., Part A: Polym. Chem.* **2008**, *46*, 2745–2754.
(15) Lligadas, G.; Percec, V. *J. Polym. Sci., Part A: Polym. Chem.* **2008**, *46*, 3174–3181.
(16) Matyjaszeski, K.; Coca, S.; Gaynor, S. G.; Wei, M.; Woodworth, B. E. *Macromolecules* **1997**, *30*, 7348–7350.
(17) Matyjaszewski, K.; Pyun, J.; Gaynor, S. G. *Macromol. Rapid Commun.* **1998**, *19*, 665–670.
(18) Otsu, T.; Yamaguchi, M. *J. Polym. Sci., Part A-1* **1968**, *6*, 3075–3085.
(19) Otsu, T.; Tazaki, T. *Chem. Express* **1990**, *5*, 801–804.
(20) Lligadas, G.; Rosen, B. M.; Monteiro, M. J.; Percec, V. *Macromolecules* **2008**, *41*, 8360–8364.
(21) Lligadas, G.; Rosen, B. M.; Bell, C. A.; Monteiro, M. J.; Percec, V. *Macromolecules* **2008**, *41*, 8365–8371.
(22) Guliashvili, T.; Percec, V. *J. Polym. Sci., Part A: Polym. Chem.* **2007**, *45*, 1607–1618.
(23) Rosen, B. M.; Percec, V. *J. Polym. Sci., Part A: Polym. Chem.* **2008**, *46*, 5663–5697.
(24) Fischer, H. *Chem. Rev.* **2001**, *101*, 3581–3610.
(25) Fischer, H. *J. Polym. Sci., Part A: Polym. Chem.* **1999**, *37*, 1885–1901.
(26) Rosen, B. M.; Percec, V. *J. Polym. Sci., Part A: Polym. Chem.* **2007**, *45*, 4950–4964.
(27) Percec, V.; Grigoras, C. *J. Polym. Sci., Part A: Polym. Chem.* **2005**, *43*, 5609–5619.
(28) Lligadas, G.; Percec, V. *J. Polym. Sci., Part A: Polym. Chem.* **2008**, *46*, 6880–6895.
(29) Bell, C. A.; Whittaker, M. R.; Gahan, L. R.; Monteiro, M. J. *J. Polym. Sci., Part A: Polym. Chem.* **2008**, *46*, 146–154.
(30) Wright, P. M.; Mantovani, G.; Haddleton, D. M. *J. Polym. Sci., Part A: Polym. Chem.* **2008**, *46*, 7376–7385.
(31) Monteiro, M. J.; Guliashvili, T.; Percec, V. *J. Polym. Sci., Part A: Polym. Chem.* **2007**, *45*, 1835–1847.
(32) Egorov, A. M.; Matyukhova, S. A. *Int. J. Chem. Kinet.* **2007**, *39*, 547–555.
(33) Egorov, A. M.; Matyukhova, S. A.; Anisimov, A. V. *Int. J. Chem. Kinet* **2005**, *37*, 296–203.
(34) Egorov, A. M.; Matyukhova, S. A.; Anisimov, A. V. *Russ. J. Gen. Chem.* **2005**, *75*, 1194–1198.
(35) Matyjaszewski, K.; Tsarevsky, N. V.; Braunecker, W. A.; Dong, H.; Huang, J.; Jakubowski, W.; Kwak, Y.; Nicolay, R.; Tang, W.; Yoon, J. A. *Macromolecules* **2007**, *40*, 7795–7806.
(36) Percec, V.; Barboiu, B.; Grigoras, C.; Bera, T. K. *J. Am. Chem. Soc.* **2003**, *125*, 6503–6516.
(37) Percec, V.; Grigoras, C.; Kim, H. J. *J. Polym. Sci., Part A: Polym. Chem.* **2004**, *42*, 505–513.
(38) Percec, V.; Grigoras, C.; Bera, T. K.; Barboiu, B.; Bissel, P. *J. Polym. Sci., Part A: Polym. Chem.* **2005**, *43*, 4894–4906.
(39) Percec, V.; Bera, T. K.; De, B. B.; Sanai, Y.; Smith, J.; Holerca, M. N.; Barboiu, B.; Grubbs, R. B.; Frechét, J. M. J. *J. Org. Chem.* **2001**, *66*, 2104–2117.
(40) Powder Metallurgy. In *In Tool and Manufacturing Engineers Handbook*, 4th ed.; Bakerjian, R., Cubberly, W. H., Eds.; Society of Manufacturing Engineers: Dearborn, MI, 1988; pp 17-1−17-42.
(41) Liou, Y. H.; Lo, S. L.; Lin, C. J. *Water Res.* **2007**, *41*, 1705–1712.
(42) Goodman, D. W. *Nature (London)* **2008**, *454*, 948–949.
(43) Valden, M.; Lai, X.; Goodman, D. W. *Science* **1998**, *281*, 1647–1650.
(44) Hughes, M. D.; Xu, Y.-J.; Jenkins, P.; McMorn, P.; Landon, P.; Enache, D. I.; Carley, A. F.; Attard, G. A.; Hutchings, G. J.; King, F.; Stitt, E. H.; Johnston, P.; Griffin, K.; Kiely, C. J. *Nature (London)* **2005**, *437*, 1132–1135.
(45) Turner, M.; Golovko, V. B.; Vaughan, O. P. H.; Abdulkin, P.; Berenguer-Murcia, A.; Tikhov, M. S.; Johnson, B. F. G.; Lambert, R. M. *Nature (London)* **2008**, *454*, 981–983.
(46) Haruta, M.; Kobayashi, T.; Sano, H.; Yamada, N. *Chem. Lett.* **1987**, *16*, 405–408.
(47) Han, J.; Liu, Y.; Guo, R. *J. Am. Chem. Soc.* **2009**, *131*, 2060–2061.
(48) Schmid, G.; Pfeil, R.; Boese, R.; Bandermann, F.; Meyer, S.; Calis, G. H. M.; Vandervelden, W. A. *Chem. Ber. Recl.* **1981**, *114*, 3634–3642.
(49) Percec, V.; Barboiu, B.; Kim, H.-J. *J. Am. Chem. Soc.* **1998**, *120*, 305–316.
(50) Lligadas, G.; Percec, V. *J. Polym. Sci., Part A: Polym. Chem.* **2008**, *46*, 4917–4926.
(51) Matyjazewski, K.; Xia, J. Fundamentals of Radical Polymerization. In *Handbook of Radical Polymerization*; Matyjaszewski, K., Davis, T. P., Eds.; Wiley-Interscience: New York, 2002; p 576.
(52) Min, K.; Gao, H.; Matyjaszewski, K. *Macromolecules* **2007**, *40*, 1789–1791.
(53) Ciampolini, M.; Nardi, N. *Inorg. Chem.* **1966**, *5*, 41.

MA8028562